Osteoarthritis and Cartilage xxx (xxxx) xxx

Osteoarthritis and Cartilage

Direct comparison of non-osteoarthritic and osteoarthritic synovial fluid-induced intracellular chondrocyte signaling and phenotype changes

B.A.C. Housmans †, G.G.H. van den Akker †, M. Neefjes §, U.T. Timur ‡, A. Cremers †, M.J. Peffers ¦, M.M.J. Caron †, L.W. van Rhijn ‡, P.J. Emans ‡, T.A.E.J. Boymans ‡, P.Z. Feczko ‡, P.M. van der Kraan §, T.J.M. Welting † ‡ *

† *Laboratory for Experimental Orthopedics, Department of Orthopedic Surgery, Maastricht University, Maastricht, the Netherlands*
‡ *Laboratory for Experimental Orthopedics, Department of Orthopedic Surgery, Maastricht University Medical Center+, Maastricht, the Netherlands*
§ *Experimental Rheumatology, Department of Rheumatology, Radboud University Medical Center, Nijmegen, the Netherlands*
¦ *Institute of Life Course and Medical Sciences, University of Liverpool, UK*

ARTICLE INFO

Article history:
Received 15 March 2022
Accepted 9 September 2022

Keywords:
Osteoarthritis
Synovial fluid
Inflammation
Fibrosis
Phenotype
Chondrocyte

SUMMARY

Objective: Since the joint microenvironment and tissue homeostasis are highly dependent on synovial fluid, we aimed to compare the essential chondrocyte signaling signatures of non-osteoarthritic vs end-stage osteoarthritic knee synovial fluid. Moreover, we determined the phenotypic consequence of the distinct signaling patterns on articular chondrocytes.

Methods: Protein profiling of synovial fluid was performed using antibody arrays. Chondrocyte signaling and phenotypic changes induced by non-osteoarthritic and osteoarthritic synovial fluid were analyzed using a phospho-kinase array, luciferase-based transcription factor activity assays, and RT-qPCR. The origin of osteoarthritic synovial fluid signaling was evaluated by comparing the signaling responses of conditioned media from cartilage, synovium, infrapatellar fat pad and meniscus. Osteoarthritic synovial fluid induced pathway–phenotype relationships were evaluated using pharmacological inhibitors.

Results: Compared to non-osteoarthritic synovial fluid, osteoarthritic synovial fluid was enriched in cytokines, chemokines and growth factors that provoked differential MAPK, AKT, NFκB and cell cycle signaling in chondrocytes. Functional pathway analysis confirmed increased activity of these signaling events upon osteoarthritic synovial fluid stimulation. Tissue secretomes of osteoarthritic cartilage, synovium, infrapatellar fat pad and meniscus activated several inflammatory signaling routes. Furthermore, the distinct pathway signatures of osteoarthritic synovial fluid led to accelerated chondrocyte dedifferentiation via MAPK/ERK signaling, increased chondrocyte fibrosis through MAPK/JNK and PI_3K/AKT activation, an elevated inflammatory response mediated by cPKC/NFκB, production of extracellular matrix-degrading enzymes by MAPK/p38 and PI_3K/AKT routes, and enabling of chondrocyte proliferation.

Conclusion: This study provides the first mechanistic comparison between non-osteoarthritic and osteoarthritic synovial fluid, highlighting MAPKs, cPKC/NFκB and PI_3K/AKT as crucial OA-associated intracellular signaling routes.

Introduction

Osteoarthritis (OA) is a debilitating disease with severe socio-economic consequences[1]. OA has been described as a multifactorial disease with common risk factors such as, age, sex, joint injury, obesity, genetic predispositions and mechanical stresses[2]. While

* Address correspondence and reprint requests to: Tim JM Welting, Laboratory for Experimental Orthopedics, Department of Orthopedic Surgery, Maastricht University Medical Center, P.O. Box 5800, 6202 AZ, Maastricht, the Netherlands. Tel.: 31-43-3884157.
E-mail address: t.welting@maastrichtuniversity.nl (T.J.M. Welting).

https://doi.org/10.1016/j.joca.2022.09.004

the exact mechanism of OA initiation remains largely unknown, a number of studies have explored the relationship between OA progression and the joint microenvironment[3,4]. A major determinant of the joint microenvironment is the synovial fluid (SF), which is present in the joint cavity[3,4]. SF ensures joint lubrication and delivery of nutrients and other essential molecules to articular cartilage[5,6]. A disturbance in SF composition might adversely affect joint homeostasis and result in OA initiation or worsening[3,4,7,8]. In general, OA synovial fluid (OASF) contains increased levels of cytokines, chemokines and damage-associated molecular patterns (DAMPs)[2]. An inflammatory joint microenvironment can compromise serum filtration by the synovium, thereby increasing plasma protein influx[9,10]. In line with this, an increased synovial fluid level of vascular endothelial growth factor (VEGF) in OA patients is known to induce vascular hyperpermeability[11]. While the compositional change of SF is evident in OA[12], only a limited number of studies investigated the direct effects of OASF on chondrocytes[8,13]. Our recent work unraveled the first key underlying mechanisms by which OASF induced chondrocyte dedifferentiation, fibrosis and proliferation[14]. As a continuation of our previous work, we aimed to compare the essential signaling and phenotypic differences of SF from human end-stage knee OA patients vs non-OA subjects on Human Articular Chondrocytes (HACs). Signaling proteins in SF were profiled using an antibody array. Chondrocyte pathway activation provoked by the two distinct SF types was explored with a phospho-kinase array. Differentially activated pathways were validated with transcription factor reporter assays. Additionally, we attempted to determine the origin of the OASF-induced signaling by comparing pathway responses of OASF and conditioned media (CM) of different OA knee joint tissues from the same patients. Ultimately, we assessed the phenotypic response and the relative importance of involved pathways for articular chondrocytes.

Materials and methods

Knee tissue collection, chondrocyte isolation, synovial fluid processing and cell culture

Human articular cartilage (HACs source), synovium, infrapatellar fat pad (IFP), meniscus and OASF were collected from total knee replacement (OA) surgery at the department of orthopedic surgery (Maastricht UMC) after written informed consent and approval by the Local Ethical Committee (METC 2017-0183). OASF was processed according to our previously published protocol[15]. Postmortem collected pure non-OASF was purchased from Articular Engineering (Illinois, USA) (details; Supplementary Table 1). OA HACs were isolated from cartilage according to a previously described procedure and cultured until passage 2 for experiments[16]. SW1353 (HTB-94, ATCC) chondrosarcoma cells were cultured in DMEM/F12 supplemented with 10% Fetal Calf Serum (FCS) and 1% Antibiotic-Antimycotic (ThermoFisher). Stimulation experiments were carried out with DMEM/F12 HEPES supplemented with either 10% (v/v) OASF or non-OASF. Pharmacological inhibitors used: 1 μM SCH7 72984 (ERKi; Bioconnect), 10 μM SB203580 (p38i; Bioconnect), 10 μM SP600125 (JNKi; Bioconnect), 10 μM Y27632 (ROCKi; Tebu-bio), 1 μM MBQ-167 (Rac/Cdc42i; Bioconnect), 1 μM Afatinib (EGFRi; Bioconnect), 1 μM Imatinib (PDGFRi; Bioconnect), 10 μM Go6976 (cPKCi; Bioconnect), 2 μM Entospletinib (SYKi; Bioconnect), 10 μM LY294002 (PI_3Ki; Bioconnect).

Antibody arrays

Signaling proteins in non-OASF (pool, $n = 7$) and OASF (pool, $n = 7$) were analyzed with the L-Series Human Antibody Array L-507 (AAH-BLG-1, RayBiotech). To explore phospho-kinase profiles, OA HACs (pool, $n = 10$, 60.000 cells/cm^2) were serum-starved for 16 h in DMEM/F12 HEPES and then stimulated for 15 min with either non-OASF (pool, $n = 7$) or OASF (pool, $n = 7$), followed by lysis with RIPA buffer (150 mM NaCl, 50 mM Tris-HCl, 5 mM EDTA, 0.5 mM DTT, 1% NP-40, 0.5% DOC, and 0.1% SDS) supplemented with cOmplete Mini protease inhibitor cocktail (Roche) and PhosSTOP™ phosphatase inhibitor cocktail (Roche). Lysates were sonicated and spun (21,380 g) for 10 min at 4°C and supernatants were stored at −80°C. Samples were analyzed by Full Moon BioSystems Inc. (Sunnyvale, CA, USA) using the phospho-explorer array (PEX100). Both increased and decreased differential protein phospho-sites with *a* >1.5-fold change were used for pathway mapping (reactome.org), as phosphorylation regulates both protein activation and inactivation[17].

Construction of reporter plasmids

Binding sequences of 11 specific transcription factor complexes (Supplementary Table 2) in front of a minimal promoter (sequence: AGAGGGTATATAATGGAAGCTCGACTTCCAG) were custom synthesized by Genecust (Boynes, France). The promoter sequences were directionally cloned into the pNL1.2 vector (Promega) through enzymatic restriction and ligation with T4 DNA Ligase (NEB). Subsequently, lentiviral constructs were generated by re-cloning pNL1.2 reporters with the In-Fusion HD Cloning Plus kit (TakaraBio) into the *Cla*I-linearized pLVX-EF1α-IRES-Puro transfer vector (TakaraBio) according to the manufacturer's instructions (primers; Supplementary Table 3). Plasmid isolation was performed with Plasmid Maxi Kit (Qiagen).

Generation of stable reporter cell lines

Lentivirus was produced by polyethylenimine-based transfection (2.5 mg/μg DNA) of pLVX-EF1α-IRES-Puro containing luciferase reporter vectors into HEK293T cells (TakaraBio) using the 4th generation lentiviral production system (TakaraBio). Viral supernatants collected after 48 and 72 h were concentrated 10 times with Lenti-X concentrator (TakaraBio) according to manufacturer's protocol. Titers were determined by p24 ELISA (Fujirebio). SW1353 reporter cell lines were generated using lentiviral transduction with 16 μg/mL DEAE-dextran (Sigma) for 8 h. Two days post-transduction, cells were selected with 2 μg/mL puromycin (Sigma). All 11 reporter cell lines were functionally validated with known positive stimuli (Supplementary Fig. 1).

Reporter gene assays

Twenty-four hours prior to the assay, SW1353 reporter cells were trypsinized (Trypsin; Thermofisher), re-seeded (60.000 cells/cm^2) into 384-well plates (Greiner Bio-One) and cultured in DMEM/F12 with 0.5% FCS. Serum-starved cells were stimulated with either 10% non-OASF (pool, $n = 7$) or OASF (pool, $n = 7$) for 6 h. In addition, 10% OASF was co-incubated with single pharmacological inhibitors or 0.1% (v/v) dimethylsulfoxide (vehicle). Lastly, cells were stimulated with either 10% tissue-CM ($n = 16$) or 10% OASF ($n = 12$) from the same donors (donor demographics; Supplementary Table 4). CM was generated from cartilage, synovium, IFP and meniscus as previously described[12]. After stimulation, cells were lysed using 15 μL Milli-Q water. Following the addition of Nano-Glo® reagent (1:1 ratio; Promega), luminescence was quantified using the Tristar2 LB942 multi-mode plate reader (Berthold Technologies)[15].

Please cite this article as: Housmans BAC et al., Direct comparison of non-osteoarthritic and osteoarthritic synovial fluid-induced intracellular chondrocyte signaling and phenotype changes, Osteoarthritis and Cartilage, https://doi.org/10.1016/j.joca.2022.09.004

RNA isolation and RT-qPCR

HACs were lysed with TRIzol reagent (ThermoFisher). Total RNA was extracted according to a previously described RNA isolation procedure[18]. Complementary DNA was generated from 500 ng RNA using M-MLV reverse transcriptase (Promega) and random hexamer priming. Real-time quantitative polymerase chain reaction (RT-qPCR) was carried out using Takyon NO ROX SYBR MasterMix dTTP blue (Eurogentec). cDNA samples (6 ng) were amplified (0.3 μM primers) and detected using a BioRad CFX96 Real-Time PCR Detection System. Amplification protocol included: 10 min denaturation at 95°C, 50 cycles of amplification (15 s denaturation at 95°C, 1 min annealing at 60°C). A list of used primers is shown in Supplementary Table 3. Data were analyzed using Biorad CFX Maestro 1.1 Software (version 4.1) according to the relative standard curve method. Gene expression was normalized to the reference gene *PPIA*.

Statistical analyses

This study used a pooled approach for both HACs (minimum of 5 donors) and SF (7 donors) to eliminate potential donor-specific variation, similar as previously published work from our group[14,19]. Sample size was based on these previous studies[14,19] and no *a priori* sample size calculation was performed. The use of non-OASF and OASF pools derived from seven different donors increased the sample volume and allowed for consistent use across variety of techniques for in-depth characterization. Data normality was assessed with the Shapiro–Wilk test. Statistical significance between two groups were calculated with unpaired student's *t* test (GraphPad Prism, version 8.0.1). As correction for multiple testing, the Holm-Sidak's Adjusted *P* Value method was applied. One-Way ANOVA followed by Dunnett's multiple comparison test was used when comparing multiple treatments to control. Kruskal–Wallis test was used when data was not normally distributed. Data were presented with individual dot plots with mean of at least three replicates ±95% confidence interval, which were considered statistically significant when $p \leq 0.05$. Statistical method and number of replicates are further specified in each figure legend.

Results

Elevated cytokine, chemokine, growth factor and DAMP levels in OASF

Signaling proteins in non-OASF and OASF were profiled by a protein-antibody array (501 proteins) and yielded 121 significantly upregulated proteins in OASF [Fig. 1(A), Supplementary Table 5]. Twenty-four proteins had higher abundance in non-OASF, but this was not significantly different. Top-ranked pathways included signaling induced by cytokines (i.e. IL16/17B/17F/23A/24/25/26 and TNF), chemokines (i.e. CCL11/24/26, CXCL1/10/12/13 and CX3CL1), growth factors (i.e. VEGFB/D, FGF8/11/20, IGF2, EGF and EREG) and DAMPs (i.e. SAA1 and S100A10/12) [Fig. 1(B), Supplementary Table 5]. These upstream signaling activators were predominantly associated with downstream MAPK, AKT and NFκB signaling [Fig. 1(B)]. Most of the screened proteins were enriched in OASF as compared to non-OASF, which is in line with an overall increased protein content in OASF [Fig. 1(C), Supplementary Fig. 2(A)]. The top 20 of significantly upregulated proteins in OASF are shown in Fig. 1(D).

Differential MAPK, RhoGTPase, AKT and NFκB signaling between non-OASF and OASF in primary chondrocytes

To explore the cellular signaling differences in HACs provoked by OASF and non-OASF, we screened for 584 phosphorylation events using a phospho-kinase array [Fig. 1(E), Supplementary Table 6]. In accordance with the signaling protein array data, pathway activity exploration revealed that OASF and non-OASF induced differential signaling in HACs that was associated with upstream activators, like tyrosine kinase-, interleukin- and toll-like receptors [Fig. 1(F)]. We identified several mediators within downstream pathways of tyrosine kinases, including MAPK (i.e. SRC, SHC1, ELK1), AKT (i.e. INSR, IRS1, AKT1, RPS6KA1) and RhoGTPase signaling (i.e. PTK2, VAV1, PAK1, WASF1) (Table I). These pathways are associated with cell cycle progression[20]. This was in accordance with the differential phosphorylation of several G1/S phase transition-associated proteins, such as CDC25A, CCND1/3, CCNB1, CDKN1B. Several signal transduction mediators downstream of interleukin- and toll-like receptor signaling were differentially regulated, including stress MAPKs (i.e. MAP2K3, MAP2K7, JUN) and NFκB-related (i.e. CHUK, NFKBIA, RELA) signaling (Table I). Downstream of toll-like receptor 4 (TLR4) signaling, differential phosphorylation of PLCG2 was found, which is known to activate both MAPK and NFκB signaling[21]. Pathway mapping further revealed AKT1 signaling downstream of tyrosine kinases- and interleukin receptors, which affected several cell survival and cell death targets, including BAD, FOXO1, and P53. In summary, differences in phosphorylation profiles in HACs provoked by non-OASF vs OASF confirm the differential AKT, MAPK and NFκB signaling as predicted by the signaling protein array. These pathways converge at the transcriptional level by regulation of FOXO1, JUN, ELK1 and RELA activity.

OASF induces MAPK, RhoGTPase, AKT and NFκB signaling stronger than non-OASF

To functionally validate the differentially regulated pathways induced by non-OASF and OASF, we analyzed the activity of 11 transcription factor complexes representative of specific pathways in SW1353 cells [Fig. 2(A)]. Both non-OASF and OASF demonstrated strong activation of the NFκB-RE, SRF-RE, SRE, AP1-RE and CRE response elements [Fig. 2(B)]. From these five response elements, NFκB-RE (1.7-fold), SRF-RE (1.5-fold), serum response element (SRE) (1.4-fold) and AP1-RE (1.3-fold) were significantly stronger induced by OASF compared to non-OASF, indicating elevated NFκB, RhoGTPase and MAPK pathway activities [Fig. 2(A) and (C)]. Additionally, small inductions were observed for non-OASF on the response elements SBE, TCFLEF-RE, and SIE [Fig. 2(B)]. TCFLEF-RE and SIE activity were significantly higher for non-OASF compared to OASF [Fig. 2(C)]. As a measure of cell cycle progression and AKT signaling, we assessed chondrocyte proliferation and protein translation activity, respectively[22,23]. OASF induced significantly more proliferation and protein synthesis than non-OASF after 2 days of stimulation (Supplementary Fig. 2(B)–(D)). Collectively, these results indicate that the pathways uncovered with both phospho-kinase and signaling protein arrays (i.e. AKT, MAPK, NFκB, RhoGTPase and cell cycle) were indeed more active upon OASF stimulation.

Pathway characterization of OASF-induced signaling

We assessed the contribution of specific pathways on the activity of the five highest activated transcription factor response

Please cite this article as: Housmans BAC et al., Direct comparison of non-osteoarthritic and osteoarthritic synovial fluid-induced intracellular chondrocyte signaling and phenotype changes, Osteoarthritis and Cartilage, https://doi.org/10.1016/j.joca.2022.09.004

elements [Fig. 2(B)] with 10 pharmacological inhibitors [Fig. 2(D)]. ERKi, p38i and JNKi greatly potentiated OASF-induced NFκB signaling [Fig. 2(E)]. Similarly, blockage of EGFR, PDGFR and PI_3K significantly increased NFκB signaling. In contrast, cPKCi resulted in an almost complete reduction (85%) of the NFκB response. Additionally, ROCKi and Rac/Cdc42i signaling diminished NFκB activity significantly. SRF transcriptional activity was diminished through ROCKi by 90%, whereas Rac/Cdc42i reduced it only by 10% [Fig. 2(B) and (E)]. Upstream mediators EGFR and SYK demonstrated signaling via SRF, as their inhibition led to significantly

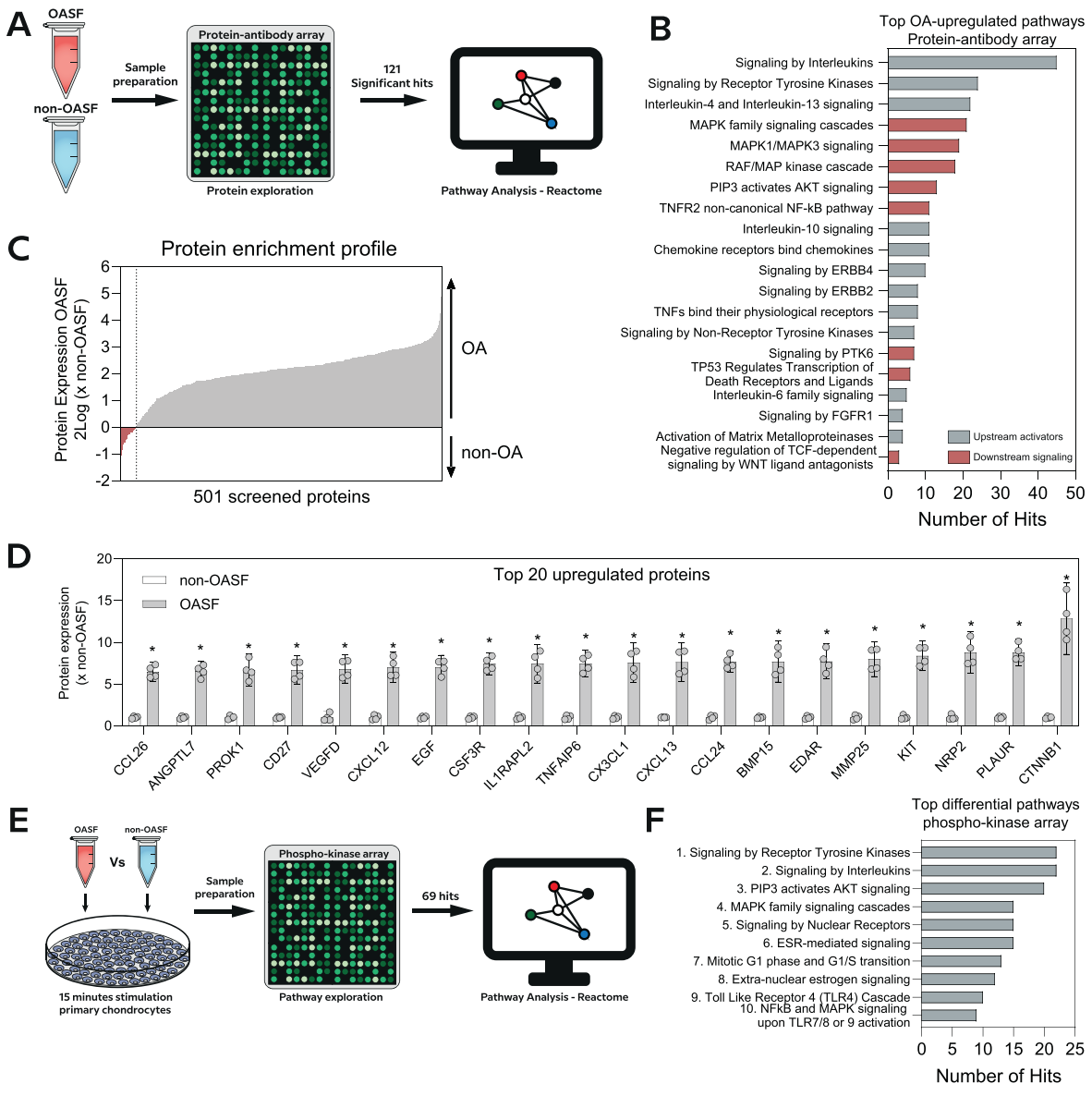

Fig. 1

Osteoarthritis and Cartilage

Top differential pathways between non-OASF and OASF. (A) A schematic representation of the experimental approach for protein profiling. Non-OASF (pool, $n = 7$) or OASF (pool, $n = 7$) were analyzed with L507 series antibody array. Statistics, multiple unpaired *t*-test (Adjusted *P* value, Holm-Sidak method), $*p < 0.05$ (mean ± 95% CI, four technical replicates). 121 significant hits were used for pathway mapping with Reactome (reactome.org). (B) Top 20 upregulated pathways by OASF. (C) Enrichment profile of the 501 screened proteins. Protein expression normalized to non-OASF. (D) Top 20 upregulated proteins in OASF ranked on highest fold change. (E) A schematic representation of the experimental approach for pathway exploration. Serum-starved OA HACs (pool, $n = 10$) were stimulated with either 10% non-OASF (pool, $n = 7$) or OASF (pool, $n = 7$) for 15 min. Pathway exploration was performed on whole-cell lysate using a phospho-kinase array. Differential proteins (FC > 1.5, increased and decreased) were used for pathway mapping with Reactome. (F) Top 10 differential pathways between non-OASF and OASF. Pathway association number of the differential proteins are indicated in Table I.

Please cite this article as: Housmans BAC et al., Direct comparison of non-osteoarthritic and osteoarthritic synovial fluid-induced intracellular chondrocyte signaling and phenotype changes, Osteoarthritis and Cartilage, https://doi.org/10.1016/j.joca.2022.09.004

reduced SRF activity. Activation of SRE exhibited clear dependency on ERK and ROCK signaling, as their inhibition reduced the OASF-induced response by at least 80% [Fig. 2(D) and (E)]. Furthermore, JNKi, Rac/Cdc42i, EGFRi, cPKCi and SYKi resulted in a significantly lower SRE response compared to OASF. On the other hand, p38i and PI_3Ki led to clear potentiation of OASF-induced SRE activation. Activation of AP1-RE depended predominantly on ERK, ROCK, Rac/Cdc42 and cPKC mediated signaling, as inhibition led to significant reductions ranging from 7 to 34% [Fig. 2(D) and (E)]. By contrast, p38i yielded a stronger OASF-induced AP1 response. To a smaller extent JNKi, PDGFRi and PI_3Ki significantly induced AP1 activity. Most pathway inhibitors (i.e. ERKi, p38i, Rac/Cdc42i, EGFRi, PDGFRi, SYKi and PI_3Ki) demonstrated clear potentiation of CRE activation compared to OASF alone, whereas JNKi reduced the OASF-induced CRE response by 2-fold [Fig. 2(D) and (E)]. Both ROCKi and cPKCi reduced the CRE response as well.

Gene Symbol	Phospho site	p-Ab/Ab		Fold change	
		OA	nonOA	OA/nonOA	Pathway Nr.
Upregulated					
ACTA1	$Tyr^{55/53}$	0.56	0.33	1.72	
ARAF	$Tyr^{301/302}$	1.04	0.61	1.70	4
BAD	$Ser^{91/128}$	1.44	0.59	2.46	3
BRCA1	Ser^{1457}	0.79	0.34	2.35	
CASP3	Ser^{150}	1.96	1.01	1.94	2
CCNB1	Ser^{126}	0.93	0.50	1.87	7
CD5	Tyr^{453}	0.24	0.14	1.70	
CDC25A	Ser^{75}	1.20	0.43	2.79	7
CHEK1	Ser^{286}	0.39	0.22	1.81	1
ELK1	Ser^{389}	0.62	0.32	1.93	1,2,5,6,8,9,10
FOXO1	Ser^{329}	0.83	0.51	1.65	2,3,4
HDAC1	Ser^{421}	0.13	0.03	4.41	3,5,6,7
IRS1	Ser^{323}	0.83	0.36	2.31	1,2,3,4
KCNA3	Tyr^{135}	1.65	0.92	1.80	
LCK	Tyr^{505}	13.16	6.47	2.04	1,2,3
LYN	Tyr^{507}	0.16	0.05	3.22	1,2,7
MAP2K3	Ser^{189}	0.73	0.45	1.63	2,9,10
MAPT	Ser^{396}	0.29	0.13	2.27	
PAK1	Ser^{141}	0.93	0.43	2.17	1,4
PLCG2	Tyr^{753}	0.79	0.40	2.01	9
RPS6KA1	Thr^{359}/Ser^{363}	0.23	0.08	2.88	1,2,9,10
SHC1	Tyr^{427}	0.47	0.25	1.91	1,2,4,5,6,8
TP53	Ser^{6}	2.32	0.89	2.61	2,3
WASF1	Tyr^{125}	1.51	0.73	2.08	1
YWHAQ	Ser^{232}	1.88	1.13	1.67	
Downregulated					
ABL1	Tyr^{204}	0.03	0.09	0.35	7
AKT1	Tyr^{474}	0.61	1.12	0.55	1,2,3,5,6,7,8
AKT1	Thr^{450}	0.53	1.00	0.53	1,2,3,5,6,7,8
CCND3	Thr^{283}	0.28	0.49	0.58	4,7
CDKN1B	Thr^{187}	0.65	1.81	0.36	3,5,6,7,8
CHUK	$Ser^{180/181}$	0.55	0.94	0.58	2,3,9,10
ESR1	Ser^{167}	0.72	1.25	0.58	1,3,5,6,8
FOXO1	$Thr^{24/32}$	0.44	0.78	0.56	2,3,4
HDAC5	Ser^{498}	0.94	1.83	0.51	3
IL3RA	Tyr^{593}	0.61	1.07	0.57	2,4
JUN	Tyr^{170}	0.70	1.19	0.58	2,3,4,5,6,9,10
MAPT	Thr^{212}	0.07	0.11	0.60	
MAPT	Ser^{356}	0.02	0.04	0.47	
MET	Tyr^{1349}	0.63	1.02	0.61	1,3,4
MYC	Thr^{58}	0.51	0.87	0.59	2,4,5,6,7
NFKBIA	Tyr^{42}	0.47	0.76	0.62	2,9,10
PTK2	Tyr^{397}	0.45	0.78	0.58	1,4,5,6,8
PXN	Tyr^{31}	0.49	1.22	0.40	1
RAF1	Ser^{296}	0.46	0.93	0.50	4
RELA	Ser^{468}	1.55	2.68	0.58	2,9,10
RPS6KB1	Ser^{418}	1.03	1.98	0.52	
SRC	Ser^{75}	0.48	0.79	0.61	1,3,4,5,6,7,8
TOP2A	Ser^{1106}	0.16	0.47	0.34	7
TP53	Ser^{33}	0.31	0.50	0.63	2,3
VAV1	Tyr^{174}	0.24	0.56	0.43	1,2,3

Table I Osteoarthritis and Cartilage

Top differential phosphorylated proteins - OASF/nonOASF

Knee joint tissues contribute to OASF-related NFκB, SIE and CRE responses

The SF composition is a result of local tissue secretion and serum-filtration[12,24]. We aimed to determine the origin of the OASF-induced signaling by investigating signaling patterns provoked by CM from meniscus, IFP, synovium and cartilage tissue in comparison to the corresponding knee SF from the same OA patients [Fig. 3(A) and (B)].

All four tissues contributed to NFκB-RE, CRE and SIE activation. IFP and synovium CM clearly provoked the highest impact on these responses [Fig. 3(A) and (B)]. Additionally, ISRE was activated by OASF and all tested CMs, except for meniscus, and presented with a relatively large donor variation in IFP and synovium CMs [Fig. 3(A) and (B)]. Both cartilage and meniscus CM slightly induced SBE activity to a similar extent as OASF, while synovium CM decreased SBE signaling [Fig. 3(A) and (B)]. NFAT5-RE exhibited clear activation upon stimulation with specific synovium and IFP CM donors [Fig. 3(A) and (B)]. Minor, but significant responses were observed for TCFLEF-RE and ARE by CM from any of the tissues and OASF, with the exception of TCFLEF-RE and ARE responses by cartilage and synovium CM, respectively [Fig. 3(A) and (B)]. While OASF convincingly induced MAPK and RhoGTPase-associated pathways, like AP1-RE, SRE and SRF-RE, none of the knee joint tissue CMs provoked a response on these reporters [Fig. 3(A) and (B)].

OASF provokes dedifferentiation, fibrosis, inflammation, catabolism and proliferation of chondrocytes

Next, we investigated the impact of the signaling differences between non-OASF and OASF on the HAC phenotype after a 24-h stimulation [Fig. 4(A)]. Cartilage-specific genes, *COL2A1* and *ACAN*, were equally expressed by both conditions, whereas other chondrogenic genes, like *COMP* (2.5-fold) and *SOX9* (4.5-fold), were strongly downregulated by OASF [Fig. 4(B)][25–27]. No differences were found between non-OASF and OASF for the expression of chondrocyte hypertrophy genes, *COL10A1* and *RUNX2* [Fig. 4(B)][13]. Expression of fibrotic collagens, such as *COL1A1*and *COL3A1*, was significantly higher in OASF-treated cells, compared to non-OASF-treated cells [Fig. 4(B)][28]. Fibrosis-associated genes, like *CEMIP* and *SRPX*, displayed lower expression in response to OASF than non-OASF, whereas S100A4 was clearly upregulated by OASF[28,29]. Typical inflammatory genes, *COX2* and *IL6*[13], were not differentially expressed between both SF origins, while a specific OASF-dependent upregulation was detected for the expression of chemokines, including *CCL2* (4.8-fold), *CXCL1* (1.5-fold), *CXCL2* (1.4-fold), *CXCL8* (1.9-fold) and *CXCL12* (3.9-fold) [Fig. 4(B)]. In contrast, *CXCL6* (2.8-fold) was higher expressed after non-OASF stimulation. Genes encoding ECM-degrading enzymes, including *MMP1* (1.5-fold), *MMP13* (3-fold) and *ADAMTS5* (1.5-fold), were significantly higher expressed in OASF-treated chondrocytes [Fig. 4(B)][30]. In contrast, *MMP2* expression was decreased by OASF compared to non-OASF[31]. OASF specifically induced the expression of proliferation-associated genes such as, *IQGAP3* (5.3-fold), *CDK1* (4.8-fold) and *CDKN3* (1.7-fold) [Fig. 4(B)][29].

Please cite this article as: Housmans BAC et al., Direct comparison of non-osteoarthritic and osteoarthritic synovial fluid-induced intracellular chondrocyte signaling and phenotype changes, Osteoarthritis and Cartilage, https://doi.org/10.1016/j.joca.2022.09.004

Characterization of OASF-induced pathway–phenotype relationship

The pathway dependency of the observed chondrocyte phenotypic responses was evaluated by pharmacological pathway inhibition [Fig. 4(A)]. ERKi significantly increased expression of *COL2A1* (1.6-fold), *ACAN* (3.2-fold) and *SOX9* (2.4-fold) [Fig. 4(C)]. ROCKi had a similar but smaller effect. JNKi resulted in the strongest upregulation (2.9-fold) of *SOX9*. Blockage of upstream kinases, EGFR and SYK, upregulated *ACAN* (1.5-fold) and *SOX9* (1.6-fold), respectively. p38i or PI_3Ki upregulated *COL10A1* by at least 2.3-fold [Fig. 4(C)]. JNK, cPKC and PI_3K pathways were uncovered as important drivers of the fibrosis-associated gene expression, since pharmacological inhibition led to significant reductions of *COL1A1*, *COL1A2*, *COL3A1*, S100A4 and *CEMIP* [Fig. 4(C)]. Additionally, SYKi downregulated CEMIP by 1.8-fold [Fig. 4(C)]. Expression of inflammatory genes was heavily dependent on cPKC signaling, since cPKCi led to transcriptional repression of all measured inflammatory genes [Fig. 4(C)]. In addition, ERKi and p38i significantly decreased *IL6, CXCL1, CXCL2,*

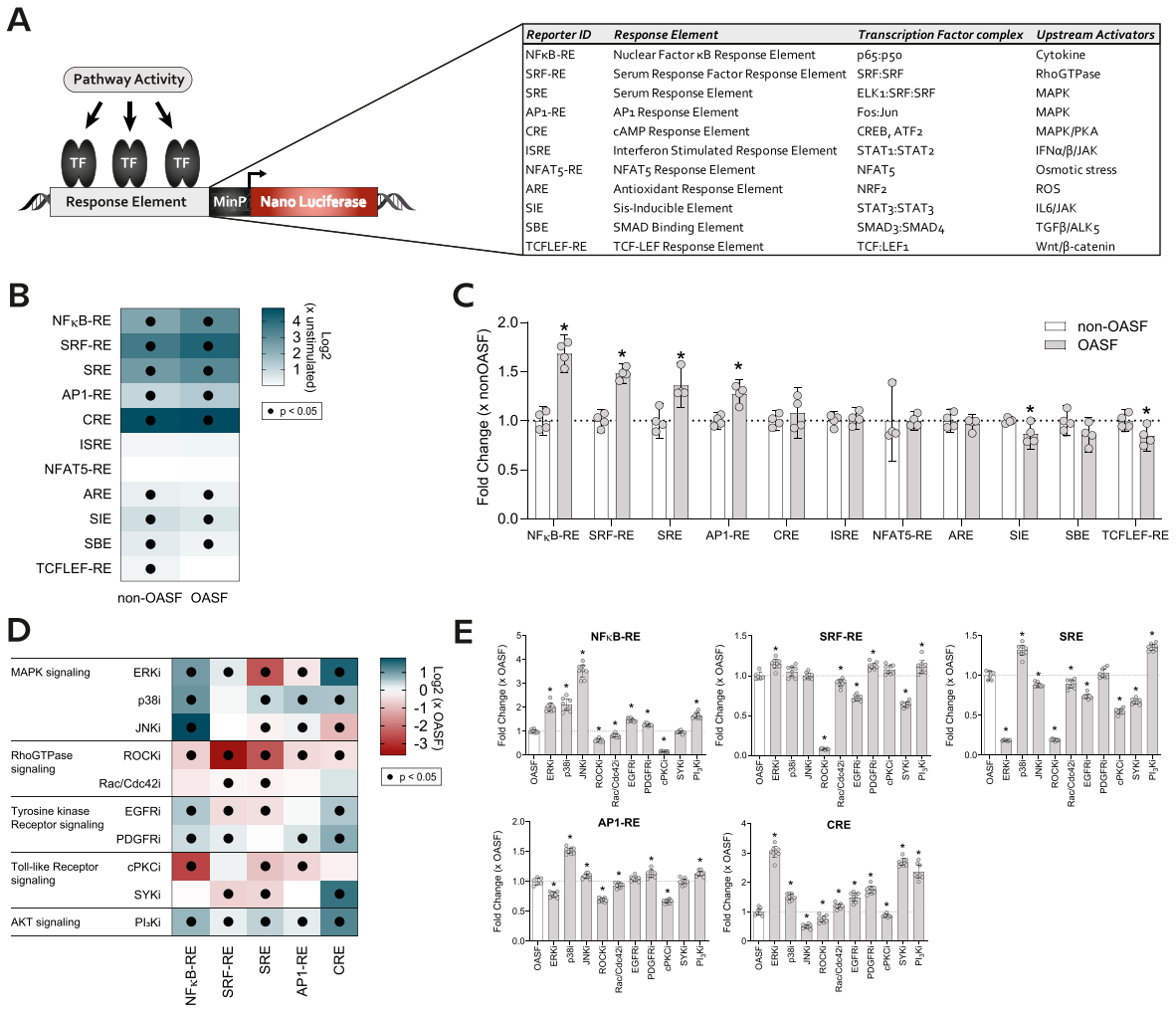

Fig. 2

Osteoarthritis and Cartilage

OASF induced stronger MAPK and inflammatory signaling than non-OASF. (A) Overview of the 11 response element driven Nano luciferases. (B) Stable reporter-expressing SW1353 cell lines were stimulated with either 10% non-OASF (pool, $n = 7$) or OASF (pool, $n = 7$) for 6 h. (B) Heatmap of non-OASF and OASF responses normalized to control (0.1% FCS). Statistics, One-way ANOVA (Dunnett's multiple comparisons test), $*p < 0.05$ (mean ± 95% CI, four technical replicates). (C) Pathway activity normalized to non-OASF. Statistics, unpaired *t*-test, $p < 0.05$ (mean ± 95% CI, four technical replicates). (D) Heatmap and (E) individual plots of SW1353 reporter lines stimulated with OASF (pool, $n = 7$) ± inhibitor (ERKi = 1 μM SCH7 72984, p38i = 10 μM SB203580, JNKi = 10 μM SP600125, ROCKi = 10 μM Y27632, Rac/Cdc42i = 1 μM MBQ-167, EGFRi = 1 μM Afatinib, PDGFRi = 1 μM Imatinib, cPKCi = 10 μM Gö6976, SYKi = 2 μM Entospletinib, PI_3Ki = 10 μM LY294002) for 6 h. Pathway activity was normalized to OASF. Statistics, One-way ANOVA (Dunnett's multiple comparisons test), $*p < 0.05$ (mean ± 95% CI, at least six technical replicates).

Please cite this article as: Housmans BAC et al., Direct comparison of non-osteoarthritic and osteoarthritic synovial fluid-induced intracellular chondrocyte signaling and phenotype changes, Osteoarthritis and Cartilage, https://doi.org/10.1016/j.joca.2022.09.004

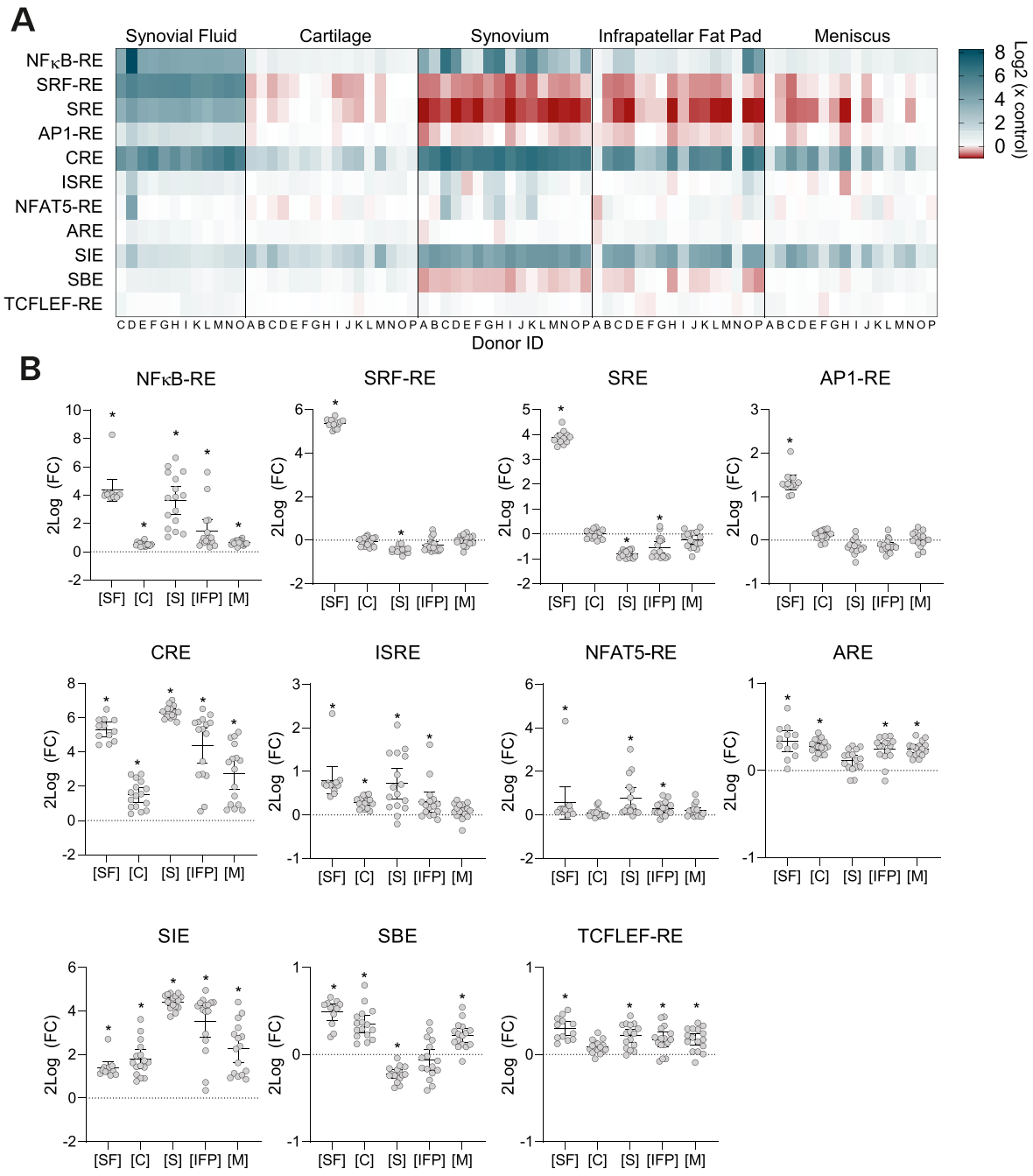

Fig. 3

Osteoarthritis and Cartilage

Joint tissue secretomes induce inflammatory signaling. Stable reporter-expressing SW1353 cell lines were stimulated with either 10% OASF (***n*** = 12 donors), cartilage-conditioned media (***n*** = 16 donors), synovium-conditioned media (***n*** = 16 donors), infrapatellar fat pad-conditioned media (***n*** = 16 donors), meniscus-conditioned media (***n*** = 16 donors) for 6 h. Pathway activity was normalized to unstimulated control (serum-free medium). (A) Heatmap and (B) scatter dot plots of donor responses (mean of 4 technical replicates) per reporter gene. Statistics, Kruskal–Wallis test (Dunnett's multiple comparisons test), ***p** < 0.05 (mean ± 95% CI, > 12 biological replicates). Individual donors indicated by unique letter (A–P).

Please cite this article as: Housmans BAC et al., Direct comparison of non-osteoarthritic and osteoarthritic synovial fluid-induced intracellular chondrocyte signaling and phenotype changes, Osteoarthritis and Cartilage, https://doi.org/10.1016/j.joca.2022.09.004

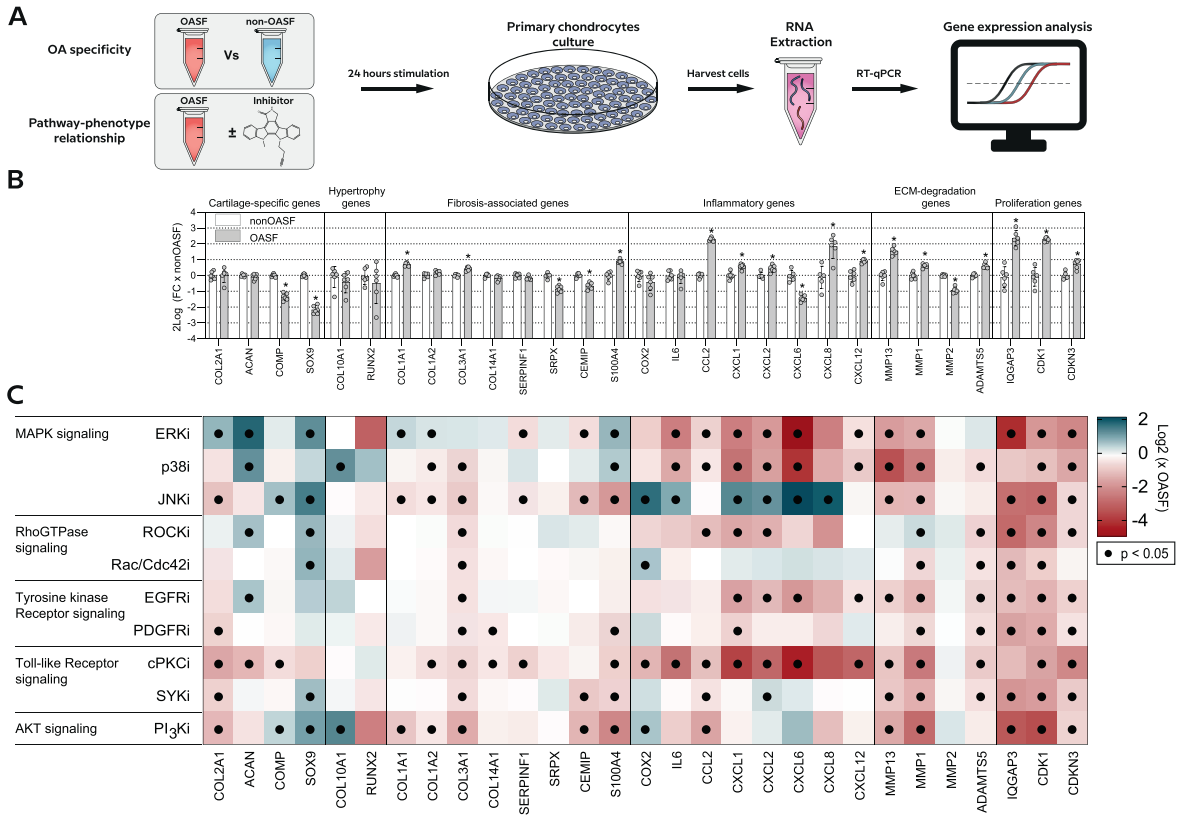

Fig. 4

Osteoarthritis and Cartilage

Phenotypical consequence of signaling differences between non-OASF and OASF. (A) OA HACs (pool, ***n*** = 5) were stimulated with either 10% non-OASF (pool, ***n*** = 7) or OASF (pool, ***n*** = 7) for 24 h. (B) Expression of phenotypic marker genes normalized to non-OASF. Statistics, multiple unpaired ***t***-test (Adjusted ***P*** value, Holm-Sidak method), ***p** < 0.05 (mean ± 95% CI, six technical replicates). (C) OA HACs were stimulated with OASF (pool, ***n*** = 7) ± inhibitor (ERKi = 1 μM SCH7 72984, p38i = 10 μM SB203580, JNKi = 10 μM SP600125, ROCKi = 10 μM Y27632, Rac/Cdc42i = 1 μM MBQ-167, EGFRi = 1 μM Afatinib, PDGFRi = 1 μM Imatinib, cPKCi = 10 μM Gö6976, SYKi = 2 μM Entospletinib, PI_3Ki = 10 μM LY294002) for 24 h. Expression normalized to OASF. Statistics, One-way ANOVA (Dunnett's multiple comparison test), ***p*** < 0.05 (mean ± 95% CI, four technical replicates).

CXCL6 and *CXCL8*, whereas JNKi demonstrated opposing effects. Most of the tested pathways (i.e. ERK, p38, JNK, EGFR, cPKC, SYK and PI_3K) demonstrated clear involvement in the regulation of *MMP1* and *MMP13* expression. p38i, cPKCi and PI_3K had the largest impact on *MMP1* and *MMP13* with downregulations ranging from 2.0 to 10.8-fold [Fig. 4(C)]. *MMP2* was not affected by any of the pathway inhibitions, whereas *ADAMTS5* was clearly diminished by cPKCi (1.8-fold), ROCKi (1.6-fold) and EGFRi (1.5-fold). To a certain degree all of the studied pathways (i.e. ERK, p38, JNK, ROCK, Rac/Cdc42, EGFR, PDGFR, cPKC, SYK and PI_3K) regulated proliferation-associated genes [Fig. 4(C)]. In particular, ERKi and PI_3Ki downregulated *IQGAP3* by 17.1- and 9.4-fold, respectively. *CDK1* was greatly affected by PI_3Ki as well (11.3-fold reduction). Lastly, both ERKi and cPKCi diminished *CDKN3* by 4.5-fold.

Discussion

The microenvironment of articular cartilage is highly dependent on the composition of the SF[3,4]. Here, we compared articular chondrocyte-integrated signaling differences provoked by OASF and non-OASF, thereby focusing on the effect of SF as whole complex fluid. Our signaling protein profiling revealed a high degree of OA-specific enrichment in cytokines, chemokines, growth factors and DAMPs. Downstream of these OASF-enriched signaling proteins, differential AKT, MAPK, RhoGTPase, NFκB and cell cycle signaling events were identified by a phospho-kinase array. Transcription factor activity analysis confirmed increased activation of NFκB, MAPK (i.e. ELK1/SRF, FOS/JUN) and RhoGTPase (i.e. SRF) signaling in OASF-treated cells. Moreover, OASF induced proliferation (i.e. cell cycle signaling) and protein translation (i.e. AKT signaling) in HACs to a larger extent than non-OASF[22,23]. Secretomes of osteoarthritic cartilage, synovium, IFP and meniscus revealed clear activation of inflammatory signaling (i.e. NFκB, SIE and CRE). Furthermore, we demonstrated that OASF-induced pathways supported chondrocyte dedifferentiation, chondrocyte fibrosis, chemokine response, production of ECM-degrading enzymes, and proliferation. In summary, our data provide new insight into the essential molecular mechanisms that drive chondrocyte phenotypic alterations mediated by the changing joint microenvironment in OA.

Please cite this article as: Housmans BAC et al., Direct comparison of non-osteoarthritic and osteoarthritic synovial fluid-induced intracellular chondrocyte signaling and phenotype changes, Osteoarthritis and Cartilage, https://doi.org/10.1016/j.joca.2022.09.004

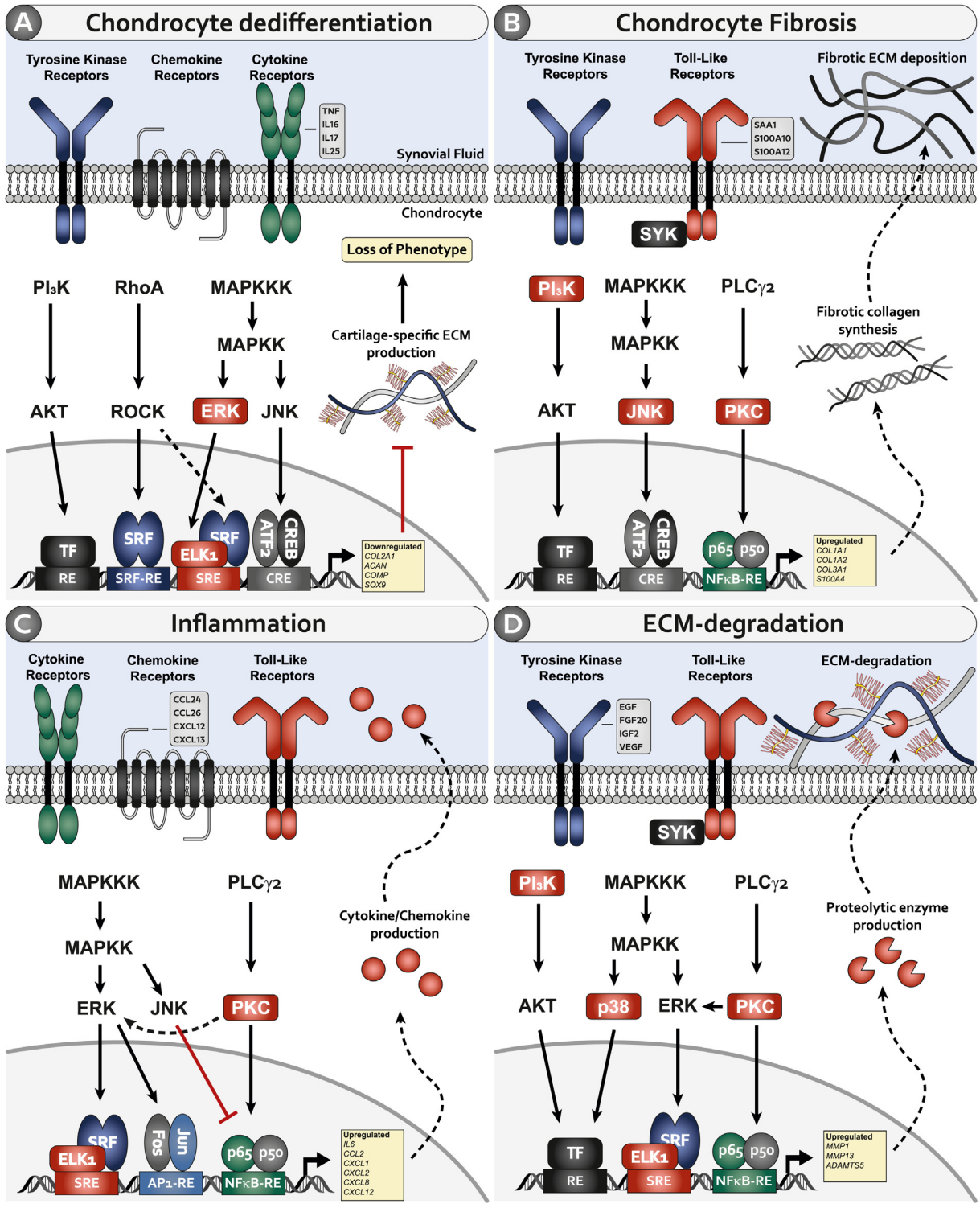

Fig. 5

Please cite this article as: Housmans BAC et al., Direct comparison of non-osteoarthritic and osteoarthritic synovial fluid-induced intracellular chondrocyte signaling and phenotype changes, Osteoarthritis and Cartilage, https://doi.org/10.1016/j.joca.2022.09.004

The composition of SF is determined by secretomes of tissues adjacent to the joint cavity and serum filtration in the synovium[12,24]. Recently, we characterized the knee joint tissue type-dependent origin of proteins in OASF[12]. Here, we compared chondrocyte signaling induced by knee OASF and secretomes of surrounding knee joint tissues. Interestingly, signaling induced by the OA tissue secretomes was restricted to inflammation-associated transcriptional activation, of which synovium and the IFP contributed the most[32–34]. Interferon-α/β (ISRE) signaling was most pronounced in synovium CM. Cartilage and meniscus secretomes activated TGFβ-related SBE signaling, which agrees with the previously reported cartilage-dependent release of TGFβ2[12]. Thus, tested joint tissues are mainly involved in the release of inflammatory mediators, which could account for the corresponding inflammatory signaling observed with OASF. A discrepancy was clearly present between OASF and the tissue secretomes regarding the MAPK and RhoGTPase signaling. AP1-RE, SRE and SRF-RE were convincingly induced by OASF, but hardly by the tissue secretomes. Since OASF is also a serum-filtrate, we speculate that the MAPK and RhoGTPase signaling by OASF originates from serum-derived molecules[35]. Indeed, increased levels of plasma proteins have been observed in OA patients as a consequence of a compromised synovial filtration[9,10]. This disease mechanism might explain the global enrichment of signaling proteins in OASF in our study.

Next, we characterized the underlying pathways and gene expression regulation of OASF-induced chondrocyte responses through pharmacological pathway inhibition. OASF-induced MAPK, AKT, RhoGTPase and NFκB signaling provoked OA-related processes (Fig. 5). In comparison with non-OASF, OASF induced a rapid loss of chondrogenic phenotype, as evidenced by dramatic *SOX9* and *COMP* downregulation. Upstream kinases, EGFR and SYK, are known to activate downstream MAPK, AKT and RhoGTPase signaling[35,36]. Suppression of the cartilage-specific phenotype was mainly mediated via ERK signaling [Fig. 5(A)], since its inhibition led to increased expression of *COL2A1*, *ACAN* and *SOX9*. ROCK signaling had resembling effects on dedifferentiation. ERK and ROCK pathways converge at the transcriptional level by activating ELK1/SRF complexes. *In vitro* chondrocyte re-differentiation was previously reported upon ERK or ROCK inhibition[26,27]. The significance of ERK signaling in OA development is further confirmed by two *in vivo* OA studies that demonstrated reduced cartilage degeneration through pharmacological inhibition of MEK-ERK signaling[37,38].

While OASF-treatment suppressed the cartilage-specific phenotype, it also promoted chondrocyte fibrosis as evidenced by upregulation of fibrotic collagen expression, when compared to non-OASF. Other fibrosis-associated genes were higher expressed by non-OASF-treated cells, whereas S100A4 was induced by OASF. Pathway characterization unveiled JNK, cPKC and PI_3K as the main signaling routes for fibrotic gene expression [Fig. 5(B)]. Both pathway mapping and literature suggests TLR4 as potential upstream activator of cPKC and JNK signaling[21,39]. TLR4 activation often occurs in tissue fibrosis[40]. Many DAMPs associated with cartilage destruction released in OASF are known to activate TLR4[41]. This includes S100A10/12 and SAA1, which we found in higher abundance in OASF, and might promote fibrotic signaling[42]. In an ovine study, fibrocartilage formation coincided with increased expression of TLR4-agonists[43].

Cytokines, chemokines and DAMPs enriched in OASF provoked an overall increased inflammatory signaling response compared to non-OASF, which led to elevated expression of several chemokine genes. In contrast, non-OASF promoted CXCL6 expression, supporting a homeostatic role for CXCL6 and loss of expression during OA progression[44]. Generally, chemokines have been associated with fibrosis in numerous tissues, and therefore might aggravate the OASF-induced fibrotic response[45]. On the other hand, chemokines play roles in the homing of mesenchymal stem cells, thereby potentially promoting cartilage repair[46]. Here, cPKC signaling was critical for activation of inflammatory NFκB-RE [Fig. 5(C)]. Additionally, ERK as target of cPKC[21] was also clearly involved in the expression of the inflammatory genes. Interestingly, JNKi potentiated OASF-induced NFκB signaling and inflammatory gene expression. One study in primary macrophages supported an anti-inflammatory role of JNK signaling via a TLR/JNK/ATF3 axis[47].

ECM-remodeling responses provoked by OASF occurred through upregulation of cartilage ECM-degenerative genes. Interestingly, *MMP2* was higher expressed by non-OASF-treated cells. While most catabolic enzymes degrade cartilage-specific ECM[30], MMP2 has been strongly associated with anti-fibrotic actions, by regulating collagen type I turnover[31]. Hence, reduced *MMP2* expression by OASF may enhance fibrosis. Pathway inhibition further revealed p38, cPKC and PI_3K as dominant signaling mediators involved in the expression ECM-degrading genes [Fig. 5(D)]. This agrees with OA studies in rodents that demonstrated attenuated cartilage degeneration through pharmacological inhibition of p38 (SB203580) or PI_3K (LY294002)[48,49].

Proliferation of articular chondrocytes was enabled by OASF, which might be caused by overall enrichment in growth factors in OASF compared to non-OASF. This could be mediated by differential phosphorylation of cell cycle proteins and upregulation of proliferation-associated genes. To some extent, all tested pathways (i.e. MAPK, RhoGTPase, cPKC, SYK and AKT) contributed to the expression of proliferation-associated genes. Proliferation coincides with loss of chondrocyte phenotype and this might function to repopulate damaged cartilage *in vivo*[50]. Recently, a proliferative potential was described as a characteristic of chondroprogenitor cells *in situ*[29] and we speculate that OASF triggers a chondroprogenitor state of the articular chondrocyte.

In conclusion, our comprehensive pathway analysis unraveled the critical difference in molecular signaling and corresponding chondrocyte phenotypic consequences between non-OASF and OASF. The scope of this study was limited to the signaling molecules present in SF, thereby eliminating the potential effects of infiltrated immune cells on chondrocyte phenotype behavior.

Our findings shed new light on the molecular signaling routes by which end-stage OASF adversely affects the chondrocyte phenotype and which may contribute to OA progression. Notwithstanding off-target effects that are inherent to pharmacological inhibitors, this *in vitro* study offers valuable insight into the OASF-induced molecular signaling routes that alter the articular

Proposed molecular mechanism of OASF-induced phenotypic processes. (A) Chondrocyte dedifferentiation predominantly driven by ERK signaling (red box) via serum response element (SRE). PI_3K, ROCK and JNK promote loss of phenotype via activation of SRF-RE and CRE. (B) Chondrocyte fibrosis mainly directed via PI_3K, JNK and cPKC signaling routes (red boxes). cPKC signaling involved via NFκB-RE activation. (C) Inflammatory response characterized by transcription of chemokine genes strongly dependent on cPKC (red box) signaling through activation of SRE, AP1-RE and NFκB-RE. ERK activation contributes to inflammatory response via SRE and AP1-RE. JNK signaling suppresses NFκB-RE activation. (D) ECM-degradation mediated primarily via PI_3K, p38 and cPKC signaling (red boxes). ERK implicated in driving ECM-degradation gene expression.

Please cite this article as: Housmans BAC et al., Direct comparison of non-osteoarthritic and osteoarthritic synovial fluid-induced intracellular chondrocyte signaling and phenotype changes, Osteoarthritis and Cartilage, https://doi.org/10.1016/j.joca.2022.09.004

chondrocyte phenotype in OA. Most significant implications were found for ERK and cPKC signaling. While ERK signaling has been well-described to negatively affect articular cartilage, cPKC has been poorly studied in this context. This study highlights a major role of cPKC for OASF-induced inflammatory responses, where previous research primarily focused on cPKC-independent inflammatory signaling, such as interleukins[34]. Future work should identify the dominant chondrocyte pathway involved in OASF-induced cPKC activation, which could be extended with *in vivo* studies to evaluate cPKC as a therapeutic target. This offers new opportunities for therapeutic strategies to counteract destructive molecular signaling in the articular joint induced by OASF.

Author contributions

BH, GA and TW contributed to study concept and design. BH, UT, AC, LR, PE, TB, TW and PF were involved in the acquisition and processing of human material. BH, GA, MN, MP and TW contributed to the data generation, analysis and interpretation. BH, GA and TW were responsible for drafting and revising the manuscript. BH, GA, MN, UT, AC, MP, MC, LR, PE, TB, PF, PK and TW contributed to manuscript editing and final approval.

Conflict of interest

The authors declare that there are no relevant conflicts of interest to report.

Role of funding source

This study was supported by a TTW Perspectief Grant: William Hunter Revisited from NWO (#P15-23) and a grant from Stichting de Weijerhorst. Mandy Peffers is funded through a Wellcome Trust Clinical Intermediate Fellowship (107471/z/15/z).

Data availability statement

The data that supports the findings of this study are available in the supplementary material of this article.

Supplementary data

Supplementary data to this article can be found online at https://doi.org/10.1016/j.joca.2022.09.004.

References

1. Salmon JH, Rat AC, Sellam J, Michel M, Eschard JP, Guillemin F, *et al*. Economic impact of lower-limb osteoarthritis worldwide: a systematic review of cost-of-illness studies. Osteoarthritis Cartilage 2016;24(9):1500–8.
2. Robinson WH, Lepus CM, Wang Q, Raghu H, Mao R, Lindstrom TM, *et al*. Low-grade inflammation as a key mediator of the pathogenesis of osteoarthritis. Nat Rev Rheumatol 2016;12(10):580–92.
3. Rohner E, Matziolis G, Perka C, Fuchtmeier B, Gaber T, Burmester GR, *et al*. Inflammatory synovial fluid microenvironment drives primary human chondrocytes to actively take part in inflammatory joint diseases. Immunol Res 2012;52(3):169–75.
4. Lewallen EA, Bonin CA, Li X, Smith J, Karperien M, Larson AN, *et al*. The synovial microenvironment of osteoarthritic joints alters RNA-seq expression profiles of human primary articular chondrocytes. Gene 2016;591(2):456–64.
5. Levick JR. Microvascular architecture and exchange in synovial joints. Microcirculation 1995;2(3):217–33.
6. Tamer TM. Hyaluronan and synovial joint: function, distribution and healing. Interdiscipl Toxicol 2013;6(3):111–25.
7. Hoff P, Buttgereit F, Burmester GR, Jakstadt M, Gaber T, Andreas K, *et al*. Osteoarthritis synovial fluid activates pro-inflammatory cytokines in primary human chondrocytes. Int Orthop 2013;37(1):145–51.
8. Barreto G, Soliymani R, Baumann M, Waris E, Eklund KK, Zenobi-Wong M, *et al*. Functional analysis of synovial fluid from osteoarthritic knee and carpometacarpal joints unravels different molecular profiles. Rheumatology (Oxford) 2019;58(5):897–907.
9. Brown DL, Cooper AG, Bluestone R. Exchange of IgM and albumin between plasma and synovial fluid in rheumatoid arthritis. Ann Rheum Dis 1969;28(6):644–51.
10. Kushner I, Somerville JA. Permeability of human synovial membrane to plasma proteins. Relationship to molecular size and inflammation. Arthritis Rheum 1971;14(5):560–70.
11. Abdel-Magied RA, AbuOmar HAS, Higazi AM, Amal A, Hassan AA. Synovial fluid level of vascular endothelial growth factor (VEGF) can predict functional status and radiological severity in patients with knee osteoarthritis (OA). Int J Clin Rheumatol 2019;14(1):10–5.
12. Timur UT, Jahr H, Anderson J, Green DC, Emans PJ, Smagul A, *et al*. Identification of tissue-dependent proteins in knee OA synovial fluid. Osteoarthritis Cartilage 2021;29(1):124–33.
13. Caron MM, Emans PJ, Surtel DA, van der Kraan PM, van Rhijn LW, Welting TJ. BAPX-1/NKX-3.2 acts as a chondrocyte hypertrophy molecular switch in osteoarthritis. Arthritis Rheumatol 2015;67(11):2944–56.
14. Housmans BAC, Neefjes M, Surtel DAM, Vitík M, Cremers A, van Rhijn LW, *et al*. Synovial fluid from end-stage osteoarthritis induces proliferation and fibrosis of articular chondrocytes via MAPK and RhoGTPase signaling. Osteoarthritis Cartilage 2022;30(6):862–74.
15. Neefjes M, Housmans BAC, van den Akker GGH, van Rhijn LW, Welting TJM, van der Kraan PM. Reporter gene comparison demonstrates interference of complex body fluids with secreted luciferase activity. Sci Rep 2021;11(1):1359.
16. Caron MM, Emans PJ, Coolsen MM, Voss L, Surtel DA, Cremers A, *et al*. Redifferentiation of dedifferentiated human articular chondrocytes: comparison of 2D and 3D cultures. Osteoarthritis Cartilage 2012;20(10):1170–8.
17. Ardito F, Giuliani M, Perrone D, Troiano G, Lo Muzio L. The crucial role of protein phosphorylation in cell signaling and its use as targeted therapy (Review). Int J Mol Med 2017;40(2):271–80.
18. Steinbusch MMF, Caron MMJ, Surtel DAM, Friedrich F, Lausch E, Pruijn GJM, *et al*. Expression of RMRP RNA is regulated in chondrocyte hypertrophy and determines chondrogenic differentiation. Sci Rep 2017;7(1):6440.
19. Caron MMJ, Ripmeester EGJ, van den Akker G, Wijnands N, Steijns J, Surtel DAM, *et al*. Discovery of bone morphogenetic protein 7-derived peptide sequences that attenuate the human osteoarthritic chondrocyte phenotype. Mol Ther Methods Clin Dev 2021;21:247–61.
20. Beier F, Loeser RF. Biology and pathology of Rho GTPase, PI-3 kinase-Akt, and MAP kinase signaling pathways in chondrocytes. J Cell Biochem 2010;110(3):573–80.
21. Asehnoune K, Strassheim D, Mitra S, Yeol Kim J, Abraham E. Involvement of PKCalpha/beta in TLR4 and TLR2 dependent activation of NF-kappaB. Cell Signal 2005;17(3):385–94.
22. Beier F. Cell-cycle control and the cartilage growth plate. J Cell Physiol 2005;202(1):1–8.
23. Katsara O, Attur M, Ruoff R, Abramson SB, Kolupaeva V. Increased activity of the chondrocyte translational apparatus accompanies osteoarthritic changes in human and rodent knee cartilage. Arthritis Rheumatol 2017;69(3):586–97.

24. Weinberger A, Simkin PA. Plasma proteins in synovial fluids of normal human joints. Semin Arthritis Rheum 1989;19(1):66–76.
25. Zaucke F, Dinser R, Maurer P, Paulsson M. Cartilage oligomeric matrix protein (COMP) and collagen IX are sensitive markers for the differentiation state of articular primary chondrocytes. Biochem J 2001;358(Pt 1):17–24.
26. Matsumoto E, Furumatsu T, Kanazawa T, Tamura M, Ozaki T. ROCK inhibitor prevents the dedifferentiation of human articular chondrocytes. Biochem Biophys Res Commun 2012;420(1):124–9.
27. Wang X, Xue Y, Ye W, Pang J, Liu Z, Cao Y, *et al*. The MEK-ERK1/2 signaling pathway regulates hyaline cartilage formation and the redifferentiation of dedifferentiated chondrocytes in vitro. Am J Transl Res 2018;10(10):3068–85.
28. Deroyer C, Charlier E, Neuville S, Malaise O, Gillet P, Kurth W, *et al*. CEMIP (KIAA1199) induces a fibrosis-like process in osteoarthritic chondrocytes. Cell Death Dis 2019;10(2):103.
29. Ji Q, Zheng Y, Zhang G, Hu Y, Fan X, Hou Y, *et al*. Single-cell RNA-seq analysis reveals the progression of human osteoarthritis. Ann Rheum Dis 2019;78(1):100–10.
30. Kevorkian L, Young DA, Darrah C, Donell ST, Shepstone L, Porter S, *et al*. Expression profiling of metalloproteinases and their inhibitors in cartilage. Arthritis Rheum 2004;50(1):131–41.
31. Ripmeester EGJ, Caron MMJ, van den Akker GGH, Steijns J, Surtel DAM, Cremers A, *et al*. BMP7 reduces the fibrocartilage chondrocyte phenotype. Sci Rep 2021;11(1), 19663.
32. Clark CA, Li TF, Kim KO, Drissi H, Zuscik MJ, Zhang X, *et al*. Prostaglandin E2 inhibits BMP signaling and delays chondrocyte maturation. J Orthop Res 2009;27(6):785–92.
33. Xin H, Wang M, Tang W, Shen Z, Miao L, Wu W, *et al*. Hydrogen sulfide attenuates inflammatory hepcidin by reducing IL-6 secretion and promoting SIRT1-mediated STAT3 deacetylation. Antioxidants Redox Signal 2016;24(2):70–83.
34. Choi MC, Jo J, Park J, Kang HK, Park Y. NF-kappaB signaling pathways in osteoarthritic cartilage destruction. Cells 2019;8(7).
35. Appleton CT, Usmani SE, Mort JS, Beier F. Rho/ROCK and MEK/ERK activation by transforming growth factor-alpha induces articular cartilage degradation. Lab Invest 2010;90(1):20–30.
36. Mocsai A, Ruland J, Tybulewicz VL. The SYK tyrosine kinase: a crucial player in diverse biological functions. Nat Rev Immunol 2010;10(6):387–402.
37. Pelletier JP, Fernandes JC, Brunet J, Moldovan F, Schrier D, Flory C, *et al*. In vivo selective inhibition of mitogen-activated protein kinase kinase 1/2 in rabbit experimental osteoarthritis is associated with a reduction in the development of structural changes. Arthritis Rheum 2003;48(6):1582–93.
38. Prasadam I, Mao X, Shi W, Crawford R, Xiao Y. Combination of MEK-ERK inhibitor and hyaluronic acid has a synergistic effect on anti-hypertrophic and pro-chondrogenic activities in osteoarthritis treatment. J Mol Med (Berl) 2013;91(3):369–80.
39. Kim HA, Cho ML, Choi HY, Yoon CS, Jhun JY, Oh HJ, *et al*. The catabolic pathway mediated by Toll-like receptors in human osteoarthritic chondrocytes. Arthritis Rheum 2006;54(7):2152–63.
40. Bhattacharyya S, Wang W, Qin W, Cheng K, Coulup S, Chavez S, *et al*. TLR4-dependent fibroblast activation drives persistent organ fibrosis in skin and lung. JCI Insight 2018;3(13).
41. Gomez R, Villalvilla A, Largo R, Gualillo O, Herrero-Beaumont G. TLR4 signalling in osteoarthritis–finding targets for candidate DMOADs. Nat Rev Rheumatol 2015;11(3):159–70.
42. Cerezo LA, Remakova M, Tomcik M, Gay S, Neidhart M, Lukanidin E, *et al*. The metastasis-associated protein S100A4 promotes the inflammatory response of mononuclear cells via the TLR4 signalling pathway in rheumatoid arthritis. Rheumatology (Oxford) 2014;53(8):1520–6.
43. Ribitsch I, Mayer RL, Egerbacher M, Gabner S, Kandula MM, Rosser J, *et al*. Fetal articular cartilage regeneration versus adult fibrocartilaginous repair: secretome proteomics unravels molecular mechanisms in an ovine model. Dis Model Mech 2018;11(7).
44. Sherwood J, Bertrand J, Nalesso G, Poulet B, Pitsillides A, Brandolini L, *et al*. A homeostatic function of CXCR2 signalling in articular cartilage. Ann Rheum Dis 2015;74(12):2207–15.
45. Sahin H, Wasmuth HE. Chemokines in tissue fibrosis. Biochim Biophys Acta 2013;1832(7):1041–8.
46. Cuesta-Gomez N, Graham GJ, Campbell JDM. Chemokines and their receptors: predictors of the therapeutic potential of mesenchymal stromal cells. J Transl Med 2021;19(1):156.
47. Thompson MR, Xu D, Williams BR. Activating transcription factor 3 contributes to Toll-like receptor-mediated macrophage survival via repression of Bax and Bak. J Interferon Cytokine Res 2013;33(11):682–93.
48. Brown KK, Heitmeyer SA, Hookfin EB, Hsieh L, Buchalova M, Taiwo YO, *et al*. P38 MAP kinase inhibitors as potential therapeutics for the treatment of joint degeneration and pain associated with osteoarthritis. J Inflamm (Lond) 2008;5:22.
49. Lin C, Shao Y, Zeng C, Zhao C, Fang H, Wang L, *et al*. Blocking PI3K/AKT signaling inhibits bone sclerosis in subchondral bone and attenuates post-traumatic osteoarthritis. J Cell Physiol 2018;233(8):6135–47.
50. Akkiraju H, Nohe A. Role of chondrocytes in cartilage formation, progression of osteoarthritis and cartilage regeneration. J Dev Biol 2015;3(4):177–92.

Please cite this article as: Housmans BAC et al., Direct comparison of non-osteoarthritic and osteoarthritic synovial fluid-induced intracellular chondrocyte signaling and phenotype changes, Osteoarthritis and Cartilage, https://doi.org/10.1016/j.joca.2022.09.004